

Morphology and Stress Study of Nanostructured Porous Silicon as a Substrate for PbTe Thin Films Growth by Electrochemical Process

Claudia Renata Borges Miranda^{a,b*}, Patrícia Guimarães Abramof^{a,c},
Francisco Cristovão Lourenço de Melo^b, Neidenêi Gomes Ferreira^{b*}

^aInstituto Nacional de Pesquisas Espaciais INPE/LAS,
C.P. 515, 122245-970 São José dos Campos - SP, Brazil

^bCentro Técnico Aeroespacial, Divisão de Materiais, AMR/IAE /CTA,
12228-904 São José dos Campos - SP, Brazil

^cCentro de Desenvolvimento de Tecnologia e Recursos Humanos, CDT,
12242-800 São José dos Campos - SP, Brazil

Received: February 17, 2004; Revised: August 3, 2004

Porous silicon layers (PSL) were produced by stain etching from a HF:HNO₃ 500:1 mixture with etching time varying in the range of 1 up to 10 min. The samples have presented nanometric porosity as a function of etching time, characteristic of heavily doped p type silicon. The residual stress and the correlation length of the layers were obtained through the analysis of the micro-Raman spectra using a phonon confinement model including a term to account for the amorphous phase. The residual compressive stress tends to increase as expected due to the contribution of smaller crystallites to be more representative as the etching time increases. PbTe thin films were electrodeposited on PSL from aqueous alkaline solutions of Pb(CH₃COO)₂, disodium salt of ethylenediaminetetraacetic acid (EDTA) and TeO₂ by galvanostatic and potentiostatic method. It was also obtained nanostructured PbTe thin films with polycrystalline morphology evidenced by X-ray Diffraction (XRD) spectra. Scanning Electron Microscopy (SEM) analysis has demonstrated good films reproducibility with an average grain size of 100 nm.

Keywords: porous silicon, electrochemical, semiconductors

1. Introduction

Porous silicon layer has been exhaustively studied since the discovery of its room temperature luminescence by Canham¹, that turns it an interesting material for device applications. The mechanism of porous silicon formation, on p or n type of monocrystalline silicon wafer, is not yet totally understood and strongly depends on the crystal doping level. In addition, the use of PS layer as a substrate may provide a key for growing narrow gap semiconductors films such as PbTe². For infrared detectors development and technology from IV-VI films the state of the art is the use of silicon substrate, that has the advantage of operate at room temperature. The main difficult of growing IV-VI films on silicon substrate is the large lattice mismatch between Si and PbTe film. This lattice parameter difference, of around 19%, leads the production of lower quality and polycrystalline films with a poor adherence. For this purpose, it is necessary to perform a systematic study to find a

suitable PS layer that releases the thermal stress and the lattice mismatch between the lead salt films and the silicon bulk for infrared detectors applications²⁻⁴.

Raman spectroscopy has demonstrated to be a powerful technique for microstructural analysis and allows the stress and correlation length determination⁵⁻⁷. Tsu *et al.*⁸ reported the first correlated study of Raman spectroscopy and photoluminescence (PL) of PSL and attributed the Raman peak shift of porous silicon to the effect of phonon confinement. Min Yang *et al.*⁹ presented a Raman scattering study that permits to extract a precise correlation between the Raman shift and the peak width. Papadimitriou *et al.*⁶ have also demonstrated the use of micro-Raman spectroscopy and the spatial correlation model to observe and separate structural and strain effects.

This work presents a morphological and structural study of nanostructured porous silicon as a substrate for PbTe thin

*e-mail: claudia@las.inpe.br, neidenei@iae.cta.br

Article presented at the II SBPMat, Rio de Janeiro - RJ, 26-29 de Outubro/2003

films growth from electrochemical technique. Micro-Raman spectroscopy and the spatial correlation model are used to estimate the residual stress of porous silicon layers obtained by stain etching, from heavily boron doped silicon wafers p^+ (100), as a function of the etching time. It is discussed the Raman peak shift and width, the amorphous silicon contribution and the correlation length for crystallites sizes of around 10 nm. This investigation was imperative for growing PbTe films on such PSL substrates by potentiostatic process and has allowed a better control of the film quality. Cyclic voltammetry was also used for studying the film deposition reaction and for finding the appropriate deposition potential range. The porous silicon and PbTe films were characterized by SEM, AFM, Raman spectroscopy, EDX and X-ray diffraction measurements.

2. Experimental

Monocrystalline p^+ type silicon (100), boron doped with concentration of 10^{18} atoms/cm³ was used for preparing PSL. Chemical etching (stain etching) was made from different concentrations of nitric and hydrofluoric acids with ratios between 50:1 and 500:1¹⁰. Strong dependence of the incubation time on the type and doping concentration of silicon wafer has been observed¹¹. This effect was minimized by adding, into the solutions, sodium-nitride with a concentration between 0.1 and 0.6 g/L in order to reduce the incubation time of PSL formation¹². The PSL morphology was analyzed by SEM with a LEO 435 system and AFM measurements with a Shimadzu SPM 9500J3 equipment by working at dynamic mode.

Lead telluride (PbTe) thin films were electrodeposited by using a solution containing dissolved TeO₂, Pb(CH₃COO)₂, and EDTA disodium salt in deionized water. The films were grown at potentials of 0.85 and 0.98 V × Ag/AgCl, confirmed by previous cyclic voltammetry measurements. The solution was formulated from 0.001 M TeO₃²⁻, 0.1 M Pb(CH₃COO)₂, and 0.13 M EDTA, which was also used to complex Pb²⁺ in order to prevent the spontaneous precipitation of Pb(OH)₂. The pH = 9 solution was adjusted with NaOH addition. At this pH tellurium is expected to be in the form TeO₃²⁻¹³.

A Microquímica MQPG-01 potentiostat with three electrode cell was used for both the cyclic voltammetry measurements and the electrodeposition of PbTe films. The electrodes were porous silicon substrates as a working electrode, Pt disk as a counter electrode and Ag/AgCl as a reference electrode. A voltage scan rate of 100 mV/s was used in cyclic voltammetry. Measurements were carried out from alkaline solutions at pH 9 containing 0.05 M PbEDTA²⁻, 0.001 M TeO₃²⁻, and mixtures of them on silicon substrates. Both electrodeposition and cyclic voltammetry were carried out at room temperature and in unstirred solutions. The

surface morphology and compositions (EDX) of the films was analyzed by SEM images using a LEO 435 system. Crystal structures were examined by a Philips PW 1830 X-ray diffractometer.

3. Results and Discussion

3.1. Residual stress in nanostructured porous silicon layers

For the stress evaluation, a single micro-Raman measurement point is not representative due to the presence of inhomogeneous stress. For this reason, we used the summation method, which consists in the summation of a large number of spectra from a selected area of the sample. In our case, five points were chosen in a central area of 4.0 mm² of the sample, and for each point the spectra were scanned five times to improve the statistics of the Raman data. Raman shift is normally used to estimate the residual stress in PSL^{5,6}. Besides, if the Raman is described theoretically, additional information can be obtained such as the crystallite size and shape, and the fraction of amorphous phase. Fig. 1 shows the Raman spectra in the vicinity of the Si peak for three porous silicon layers samples with etching time of 2, 5 and 8 min. The spectrum corresponding to the monocrystalline silicon is also plotted in the figure as a reference (solid line). A broadening and an asymmetry can be observed in the Raman spectra of the PSL compared to the monocrystalline Si peak.

Raman spectra of PSL was analyzed by using a correlation length model developed by Richter *et al.*¹⁴. In this model, disorder or finite size effects may result in a relaxation of the momentum conservation rule leading to a downshift and

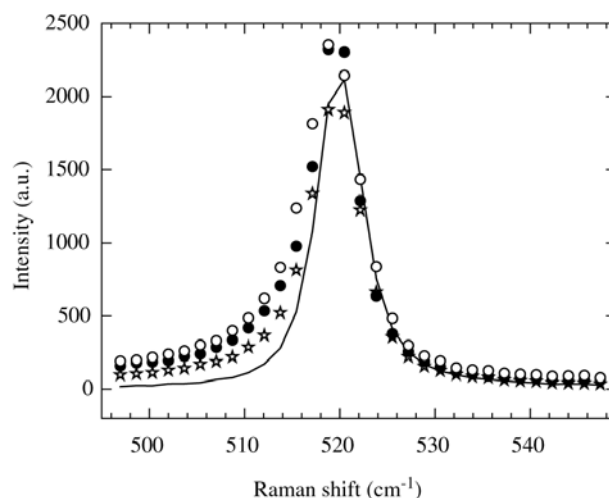


Figure 1. Raman spectra measured in the vicinity of the Si peak for PS layers samples with 1(stars), 5 (open circles), and 8 (closed circles) min of etching time. The solid line represents the spectrum of monocrystalline silicon.

an asymmetric broadening of the first order Raman peak. This model was improved afterwards by Campbell and Fauchet⁷ to calculate separately the correlation length L for three micro-crystals shapes, namely: spherical, columnar and thin slab. The intensity of the first order Raman band of porous silicon is calculated by the sum of two components: a band given by the phonon confinement model (Richter) and a Gaussian distribution to account for amorphous silicon^{5,15} through the following relation:

$$I(\omega) = A \int \frac{|C(q)|^2 d^3q}{(\omega - \omega(q))^2 + (\Gamma_0/2)^2} + \frac{B}{\Gamma_a \sqrt{\pi/2}} \exp\left(-2 \frac{(\omega - \omega_a)^2}{\Gamma_a^2}\right) \quad (1)$$

where $\omega(q) = \omega_0 - 120(qa_0/2\pi)^2$ is the phonon dispersion relation, q is the wave vector, $a_0 = 0.356$ nm is the lattice parameter of bulk silicon, $\Gamma_0 \sim 4.5 \text{ cm}^{-1}$ is the Raman intrinsic line width of crystalline silicon, $\omega_0 = 520.5 \text{ cm}^{-1}$ is the wave number of the first order Raman band in the absence of disorder effects and stress effects, and $C(q)$ are the Fourier coefficients of the phonon confinement⁷. The Fourier coefficients are given as a function of the correlation length or the theoretical crystal size L . The Gaussian band shape corresponding to the amorphous silicon is centered at ω_a with a full width at half maximum Γ_a .

The Raman spectrum of each sample of the set of PS layers with etching time varying from 1 to 10 min was fitted by the expression described above, assuming a columnar crystallite shape. The correlation length (L), the linewidth (Γ_0), the frequency shift (ω_0), the linewidth and the frequency shift of the amorphous silicon were used as free parameters for the fitting. The columnar crystallite size decreases from 13 to 9 nm as the etching time increases from 1 to 10 min. The residual stress can be obtained from the difference between the observed frequency of the first order Raman peak (ω_{obs}), which is shifted in relation to the crystalline Si natural frequency (ω_0), and the confinement frequency (ω_{conf}) obtained from the theoretical evaluation of the Raman spectrum. Therefore, the stress induced shift is given by⁶

$$\Delta\omega_{\text{stress}} = \omega_{\text{obs}} - \omega_{\text{conf}} \quad (2)$$

Figure 2 depicts the stress induced shift for the porous silicon samples as etching time increases. Note that the stress induced shift increases as the correlation length decreases. However, the stress induced shift does not have a monotonic behavior for etching times higher than 4 min, where is observed an oscillation in the induced stress shift.

The morphology of PSL was also observed by AFM analysis. Details of this subject were discussed in a previ-

ous work¹⁶. The nanocrystalline size and size distribution depend on the experimental parameters such as substrate level doping and type and also the acid concentration. A characteristic of p^+ type silicon, heavily doped, is the formation of a columnar-type structure of few nanometers. For few min of etching time it was observed just a small roughness correspond to the initial stage of the etching and a nanoporous formation. The samples presented a non-uniform porous distribution with crystallites sizes of around 10 up to 40 nm. In fact, AFM images revealed a fractal structure of the surface more and more inhomogeneous as the etching time increases. This behavior was attributed a simultaneous and competitive process while the crystallites become larger because new smaller crystallites always will appear during the etching. This observed morphology variation confirms the oscillation behavior for induced stress from Raman spectra evidenced in Fig. 2. These results were also confirmed by X-ray diffraction and reflectivity techniques for strain and porosity evaluation on PSL described elsewhere¹⁷.

3.2. PbTe electrodeposition

The process for obtaining semiconductors films by electrodeposition presents many advantage compared to the conventional techniques for epitaxial growth. This is a simple and low cost thin film method¹⁸. Electrodeposition can be carried out using substrates with different sizes and shapes. Reactions involved occur closer to the equilibrium and the deposition process may be controlled more easily than in many high temperature gas phase methods as HWE or Fresh Evaporation. Besides, it is not necessary the use of toxic gaseous precursors unlike in chemical gas phase methods. The only major limitation of electrodeposition is the use of a conductive substrate, which is eliminated in the

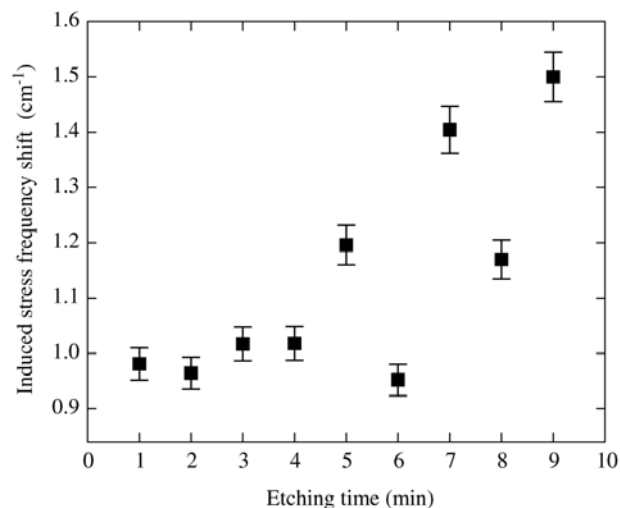


Figure 2. Stress induced shift (squares) as a function of the etching time.

case of PSL. Some authors^{13,19,20} have studied the PbTe electrodeposition by using different substrates. It was also made cyclic voltammetry measurements for studying the film deposition reactions. This study was important for analyzing the reduction/oxidation peaks of lead and tellurium. The results have shown that the work potential range between -0.7 to $-0.95 \text{ V} \times \text{Ag/AgCl}$ correspond to the necessary potential for the film growth.

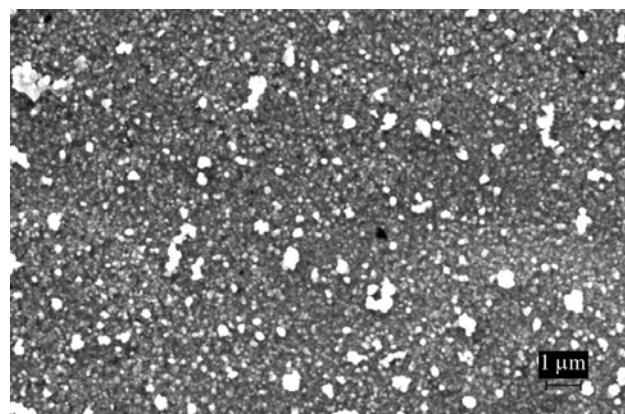
PbTe thin films were deposited by using PSL as work electrode, Pt disk as a counter electrode and a reference electrode of Ag/AgCl. The potential range that promote epitaxial growth is very narrow (0.05 V) and a very small current variation provokes too large a potential variation. Potentiostatic growth in the range of -0.85 and $-0.98 \text{ V} \times \text{Ag/AgCl}$ are closer to lead oxidation potential and has permitted a better deposition control. SEM surface morphology of the PbTe film electrodeposited on PSL substrates etched during 3 min has evidenced a polycrystalline and nanostructured grains with an average size of 100 nm. The images on Figs. 3a and 3b correspond to films grown during 30 min by potentiostatic mode with $0.98 \text{ V} \times \text{Ag/AgCl}$. The white regions on the figures also present a PbTe film composition confirmed by EDX analysis.

X-ray diffraction measurements allow us to obtain quantitative information about the epitaxial growth deduced from a large surface area. X-ray diffraction spectra for PbTe films are shown on Fig. 4. The films presented a polycrystalline structure and can be observed the PbTe peaks (200), (220), (222) e (400). It is also observed lead peak. For films grown from potentiostatic process this lead peak present less intensity and did not appear in some films. These spectra are similar to the PbTe films on SnO_2 obtained by Saloniemi *et al.*¹³ and refer to the cubic PbTe. This lead contamination is probably due to the films to be formed in the higher negative potential that makes favorable only the lead deposition. This result confirm that the control of deposition potential strongly affect the film stoichiometry.

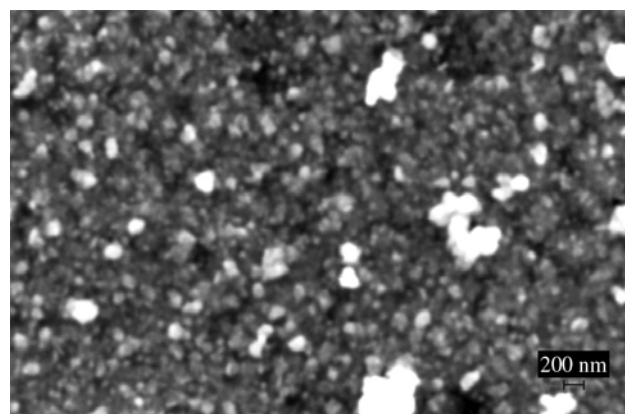
4. Conclusions

Raman spectroscopy was used as a suitable technique for establishing the relationship between the Raman peak shift and peak width for PS layers. From the measured spectra the residual stress was evaluated as a function of the etching time. The competitive process between the increase of the crystallites and surface porosity is detected by the Raman spectra and gives a significant contribution when the density of smaller crystallites is higher and depends on the etching stage for each sample analyzed. The results also evidence an almost constant and small residual stress values for the first 4 min of etching time, originated from nanostructures of singular uniformity.

PbTe thin films were deposited potentiostatically by



(a)



(b)

Figure 3. SEM images for PbTe thin films electrodeposited on PSL etched during 3 min at potential of $0.98 \text{ V} \times \text{Ag/AgCl}$. a) 6.000 X; b) 18.000 X.

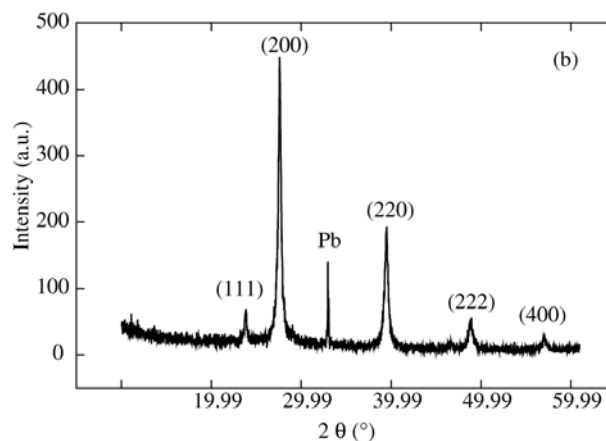


Figure 4. X-ray diffraction of PbTe thin film electrodeposited at potential of $0.98 \text{ V} \times \text{Ag/AgCl}$ by potentiostatic process on PSL etched during 3 min.

electrochemical process on PSL with a relative success. For potentiostatic process the film growth was carried out at potentials of 0.85 and 0.98 V \times Ag/AgCl. The films presented polycrystalline morphology with a strong dependence of the deposition rate, controlled by the range of deposition potential that influences the film epitaxy. It was not observed a preferential orientation from X-ray diffraction measurements besides the identification of lead peaks. The results may be considered promising by to be an innovative process for growing PbTe films. This work associated the use of PSL for obtaining a PbTe and minimizing the intrinsic stress in such a film usually presents when monocrystalline silicon is used as substrate.

References

1. Canham, L.T. *Appl. Phys. Lett.*, v. 57, n. 10, p. 1046-1048, 1990.
2. Zimin, S.P.; Preobrazhensky, M.N.; Zimin, D.S. *et al.*, *Infrared Phys. and Technol.* v. 40, p. 337-342, 1999.
3. Bondarenko, V.P.; Vorozov, N.N.; Dikareva, V.V. *et al.*, *Technol. Phys. Lett.*, v. 20, n. 10, 51-55, 1994.
4. Zimin, S.P.; Zimin, D.S.; Saunin, I.V. *et al.*, *Inorganic Mat.*, v. 34, n. 5, p. 440-441, 1998.
5. Manotas, S.; Agulló-Rueda, F.; Moreno, J.D.; Ben-Hander, F.; Guerrero-Lemus, R.; Martínez-Duart, J.M., *Phys. Stat. Sol.*, v. 182, p. 245-248, 2001.
6. Papadimitriou, D.; Bitsakis, J.; López-Villegas, J.M.; Samitier, J.; Morante, J.R.; *Thin Solid Films*, v. 349, p. 293-297, 1999.
7. Campbell, I.H.; Fauchet, P. M. *Solid State Commun.*, v. 58, n. 10, p. 739-741, 1986.
8. Tsu, R.; Shen, H.; Dutta, M. *Appl. Phys. Lett.*, v. 60, n.1, p. 112-114, 1992.
9. Yang, M.; Huang, D.; Hao, P.; Zhang, F.; Hou, H.; Wang, X. *J. Appl. Phys.*, v. 75, n. 1, p. 651-653, 1994.
10. Vazsonyi, É.; Szilágyi, E.; Petrik, P.; Horváth, Z.E.; Lohner, T.; Fried, M.; Jalsovszky, G. *Thin Solid Films*, v. 388, p. 295-302, 2001.
11. Steckl, A.J.; Xu, J.; Mongul, H.C.; Mogren, S. *Appl. Phys. Lett.*, v. 62, n. 16, p. 1982-1984, 1993.
12. Kelly, M.T.; Chun, J.K.M.; Bocarsly, A.B. *Appl. Phys. Lett.*, v. 64, n. 13, p. 1693-1695, 1994.
13. Saloniemi, H.; Kanninen, T.; Ritala, M.; Leskela, M. *Thin Solid Films*, v. 326, p. 78-82, 1998.
14. Richter, H.; Wang, Z.P.; Ley, L. *Solid State Commun.*, v. 39, n. 5, p. 625-629, 1986.
15. Sui, Z.; Leong, P.P.; Herman, I.P.; Higashi, G.S.; Temkin, H. *Appl. Phys. Lett.*, v. 60, n. 17, p. 2086-2088, 1992.
16. Abramof, P.G.; Ferreira, N.G.; Beloto, A.F.; Ueta, A.Y. *Journal of Non-Crystalline Solids*, v. 338-340, p. 139-142, 2004.
17. Abramof, P.G.; Ferreira, N.G.; Beloto, A.F.; Ueta, A.Y. *10th ISMANAN, Foz do Iguaçu, Brazil*, p. 110-111, August/2003.
18. Rajeshwar, K. *Adv. Mater.*, v. 4, n. 1, p. 23-29, 1992.
19. Dimova-Malinovska, D.; Sendova-Vassileva, M.; Kamenova, M.; Tzenov, N.; Tzolov, M. *Vacuum*, v. 47, n. 9, p. 1133-1138, 1996.
20. Saloniemi, H.; Kemel, M.; Ritala, M.; Leskela, M. *J. Electroan. Chem.*, v. 482, p. 139-148, 2000.

